

VENTILATED FLOWS WITH HYDROFOILS

By Kenneth L. Wadlin

National Aeronautics and Space Administration  
Langley Field, Va.

Presented at the Twelfth General Meeting of the  
American Towing Tank Conference,  
University of California

Berkeley, California  
August 31 - September 2, 1959

LIBRARY COPY

JUL 10 1959

IN  
LIBRARY  
LANGLEY FIELD, VIRGINIA

REPRODUCED FROM BEST AVAILABLE COPY

FACILITY FORM 602  
N 66-86294  
(ACCESSION NUMBER)  
32  
(PAGES)  
TMX-57843  
(NASA CR OR TMX OR AD NUMBER)

(THRU)  
None  
(CODE)  
(CATEGORY)

807-39875

## VENTILATED FLOWS WITH HYDROFOILS

Kenneth L. Wadlin

Langley Research Center  
National Aeronautics and Space Administration

## I ABSTRACT

It has been observed in experimental investigations involving ventilated flows with submerged hydrofoils that complete ventilation becomes increasingly difficult to obtain as the speed and depth of submergence of the hydrofoil are increased. An exploratory investigation of this difficulty has shown that the spray sheets that form above the water surface, on blunt struts intended to induce ventilation, are the primary cause of the limited ventilation. Because of the relatively low momentum in these spray sheets they are drawn together by small pressure differentials created by the air in the cavities being carried away by entrainment in the water.

It has been shown that the degree of ventilation can be appreciably increased by using small deflectors to apply an outward velocity to the spray sheets. However, complete ventilation was not realized and it appears such ventilation may only be possible at relatively shallow submergences.

## II INTRODUCTION

Ventilation is an interesting and important flow phenomenon which has been associated with hull steps for some time. However, only

recently with the renewed interest in hydrofoil supported craft and the advent of hydro-skis has much effort been made to understand it. By ventilation is meant the entrance of air from the atmosphere to low pressure areas on lifting surfaces or bodies operating in water. Interest in ventilation has been primarily in connection with seaplane hull steps, hydrofoils, hydro-skis, and submerged bodies. However, ship hulls, rudders, and propellers are also susceptible to this phenomenon.

When ventilation occurs, areas which previously were experiencing low pressures are subjected to the relatively high atmospheric pressure or pressures approaching atmospheric pressure. This results in significant changes in the flow patterns and the force characteristics of the elements involved. These force changes may result only in a simple change in static equilibrium. However, in many cases the flow reverts to the unventilated condition before equilibrium is reached and instability occurs. Such instabilities may be manifested as porpoising or skipping of a seaplane, heaving, yawing or stumbling of a hydro-ski or hydrofoil-equipped craft or vibration of propellers and rudders.

Ventilation is also of interest in connection with supercavitating hydrofoils operating near the water surface since the fully ventilated condition is analogous to the zero cavitation number case. As a matter of fact data for the zero cavitation number case are obtained in towing tanks by inducing ventilation. The cavitation number is the parameter

defining cavity flow and is  $\sigma = \frac{P_0 - P_c}{q}$  where  $P_0$  is the free-stream

static pressure,  $p_c$  is the pressure in the cavity, and  $q$  is the free-stream dynamic pressure. In unventilated cavity flow, where  $p_c$  is equal to the vapor pressure of water, zero cavitation number requires the dynamic pressure to be infinite which means infinite speed. When the cavity is vented to the atmosphere,  $p_c$  is atmospheric pressure or at shallow drafts equal to  $p_0$  and the cavitation number is zero.

The lift-drag ratios of hydrofoils designed for supercavitating flow are generally depreciated if operated in the fully wetted condition. Therefore early ventilation may be of interest for efficiency as well as stability reasons when supercavitating hydrofoils are required for high-speed applications. Ventilation may also be used to provide flow similarity with Froude models in towing tanks. This paper is primarily concerned with the case of a fully submerged supercavitating hydrofoil operating in the ventilated condition. In particular, flow conditions which influence the degree of ventilation of the hydrofoil are discussed.

### III EXAMPLES OF VENTILATION

It has been established (ref. 1) that low pressure on a hydrofoil is not a sufficient requirement for ventilation but that separation of the hydrofoil boundary layer is also required. It has also been found that separation of the boundary layer is greatly retarded by the presence of the free water surface.

On surface piercing hydrofoils and struts ventilation generally occurs, as might be expected, by air entering along the hydrofoil from

the water surface. Experimental studies in connection with this type of ventilation have been carried out by several investigators (see refs. 1 to 6). Figure 1 is an example of such a hydrofoil that has ventilated. The photograph is of a surface piercing dihedral hydrofoil having an NACA 64A-series airfoil section. It can be seen that the ventilated area extends from the water surface to a point near the tip of the hydrofoil. In reference 1 this region was shown to be the extent of the area of boundary-layer separation. Ventilation in this case started at the water surface when the separated area extended to the water surface and rapidly travelled toward the tip of the hydrofoil. The cavity on the hydrofoil is open directly to the atmosphere and is very long.

On fully submerged lifting surfaces, however, ventilation has been found to occur through the trailing vortices. In such cases the air is fed to the low pressure separated areas on the lifting surface through paths provided in the vortex core. Ventilation through the vortices has been investigated in connection with experimental studies of hydro-skis operating in the fully submerged condition (refs. 7 to 9). Figure 2 shows development of vortex ventilation on a flat plate having an aspect ratio of 0.25. The upper photograph shows the flow after the low pressure in the vortex core has vented to the atmosphere. The air appears to enter the vortex at the turbulent area at the base of the roach and extends to a point well forward but not in contact with the plate. The lower photograph shows the flow after the aeration of the vortex core

had moved progressively forward until it contacted the separated area on the plate and complete ventilation occurred. The flow has separated completely from the leading edge of the surface and the cavity is open to the atmosphere.

Ventilation through the separated area behind a blunt-based strut has been used in connection with experimental studies of supercavitating hydrofoils operating in the fully submerged condition. In these studies experimental data were being obtained for correlation with a recently developed theory (ref. 10) for calculation of the force characteristics of supercavitating hydrofoils at zero cavitation number. Zero cavitation number was obtained by increasing the cavity pressure to atmospheric pressure by inducing ventilation. To accomplish this the hydrofoils were mounted on a blunt-based parabolic strut. The separated area at the base of the strut results in a ventilated cavity behind the strut. When a supercavitating hydrofoil is mounted on such a strut the cavity behind the strut provides a path for large quantities of air to enter the low pressure vapor cavity developed by the hydrofoil. If the vapor cavity were not ventilated, it would be limited in size as shown in the photograph of figure 3. Both photographs in figure 3 were taken simultaneously. The upper one was taken from above the water surface and the lower one is an underwater side view. The hydrofoil is mounted on a streamlined strut which does not provide a path for air to reach the vapor cavity. As shown in figure 4, when a path for atmospheric air is provided by the use of a blunt-based parabolic strut, the cavity produced

by the hydrofoil expands. This occurs since the cavity pressure is now increased from vapor pressure of about 50 pounds per square foot to atmospheric pressure of about 2,120 pounds per square foot. Correspondingly the cavitation number changes from 0.19 to zero.

#### IV INCOMPLETE VENTILATION

In the investigation mentioned above the correlation between theory and experiment was not as good at the higher speeds and greater depths of submergence as it was in the lower ranges of these parameters. Measurements of the cavity pressures showed these pressures to be less than atmospheric for these higher range conditions. The cavitation numbers based on these measured cavity pressures were, of course, greater than zero and resulted in force characteristics different from those predicted by the theory for the zero cavitation number case, and the data were not suitable for direct correlation with the theory.

When the ventilated submerged lifting surface is operating near the free water surface the cavity can readily intersect the water surface and gain complete access to the atmosphere. The flow for such a condition is shown in the lower photograph of figure 2. However, as the submergence of the lifting surface increases, the cavity length required to reach the water surface increases and it becomes increasingly difficult for the cavity to gain complete access to the atmosphere. Therefore at the deeper submergences the role of the blunt strut to provide a path for the ventilating air increases to the point where all the air

entering the hydrofoil cavity enters through the cavity provided in the strut wake.

Since the cavity behind the strut was the passage through which air must flow to the hydrofoil cavity it was apparent that this path was inadequate. Since the pressure at the water surface is atmospheric, it had been considered the cavitation number here would be zero and the cavity therefore would theoretically be infinitely long. Such cavities have been approximated behind cylinders, blunt-based struts, and surface-piercing hydrofoils and would be expected to provide ample ventilation. Photographs of the flow such as that presented in figure 5 revealed that this was not the case. Instead of a cavity with a large open length at the water surface as expected, the cavity profile was inverted with a small open length occurring at the water surface. Such a stricture in the path for the ventilating air would be expected to cause the limited ventilation being experienced.

## V VENTILATION STRICTURE

The relatively thin film of water running up the sides of the strut above the water surface appeared to be the most probable cause of this stricture in the ventilation path. Since air is being entrained in the cavities behind the strut and the hydrofoil, there must be a flow of air into the cavity. This flow can not occur without a pressure difference; therefore, the pressure in the strut cavity is less than atmospheric. This being the case there is a pressure differential operating on the



spray sheets coming off the strut and forming the mouth of the cavity. This pressure differential would tend to bring the spray sheets together. The pressure differential (see fig. 6) between the atmospheric pressure  $p_o$  and the cavity pressure  $p_c$  acts normal to the spray sheet of width  $w$  and mass density  $\rho$ . The pressure differential accelerates the sheet toward  $p_c$ . This acceleration is:

$$a = \frac{p_o - p_c}{\rho w} \quad (1)$$

and is constant. The acceleration of a particle in a curved path is:

$$a = \frac{V^2}{R} \quad (2)$$

where  $V$  is the velocity of the particle and  $R$  is the radius of its path so:

$$\frac{p_o - p_c}{\rho w} = \frac{V^2}{R} \quad (3)$$

Equation (3) may be rewritten as:

$$\frac{2(p_o - p_c)}{\rho V^2} = \frac{2w}{R} \quad (4)$$

where the first term is the cavitation number  $\sigma$ . This gives

$$R = \frac{2w}{\sigma} \quad (5)$$

Assuming  $V$ ,  $(p_o - p_c)$ , and  $w$  to be constant for a given elevation on the spray sheet,  $R$  will be constant so the path will be a circle and:

$$x = \sqrt{R^2 - y^2} \quad (6)$$

The length of the cavity enclosed by the spray sheet at a given elevation is the value of  $x$  where  $y = R - \frac{t}{2}$  therefore:

$$x_c = \sqrt{Rt - \frac{t^2}{4}} \quad (7)$$

Combining equation (7) with equation (5) gives:

$$x_c = \sqrt{\frac{2wt}{\sigma} - \frac{t^2}{4}}$$

or

$$\frac{x_c}{t} = \sqrt{\frac{2(w)}{\sigma(t)} - \frac{1}{4}}$$

This relationship is presented graphically in figure 7. It can be seen that the length of the cavity behind a strut may be quite limited for what would appear to be reasonable spray thicknesses. Also it should be noted that at a given speed if the air entrainment rate in the cavity should increase the cavity pressure will decrease causing an increase in cavitation number and a consequent reduction in the air passage area at a time when more air is required. However, this reduction in pressure will generally result in an increased velocity of the air entering the cavity to compensate in some degree for the decrease in area.

## VI EXPERIMENTAL INVESTIGATION

In an effort to better understand the causes of the ventilation stricture an exploratory experimental investigation was made in tank no. 1

and the high-speed hydrodynamics facility at the NASA Langley Research Center. The hydrofoil and strut shown in figure 8 were towed at speeds up to 250 feet per second at angles of attack of  $4^\circ$  and  $8^\circ$  and at depths of submersion of 0.5, 1.0, and 1.5 hydrofoil chords. Underwater and above water photographs were taken of the cavity flows. Pressures at the base of the strut were measured by means of wire strain-gage pressure transducers in conjunction with short air-filled tubes having orifices at the locations shown in figure 8.

The fact that the spray sheet closes and results in a stricture in the ventilating path is shown in the sequence photographs of figure 9. The hydrofoil is at an angle of attack of  $8^\circ$  and at a depth of submergence of 1.0 hydrofoil chord. The first photograph (12 fps) shows the separated spray sheets coming off the sides of the strut. The base of the hydrofoil and its trailing vortices are ventilated by air flowing through the cavity formed behind the strut. At 13 fps the spray sheets have drawn together at a point close to the base of the strut. The cavity below the water surface was apparently not significantly influenced by this extent of stricture. At 14 fps the spray sheets have drawn together at a point still closer to the strut. At 15 fps the spray sheets appear to have drawn together almost immediately behind the strut. Apparently at 12 fps the air being entrained in the strut and hydrofoil cavities was small enough to be readily supplied with little pressure differential required to carry it into the cavities. The cavity pressure therefore is essentially atmospheric and the cavitation number is essentially zero. As

the speed increases the entrainment rate is increased so that more air is required. The demand for more air results in a pressure drop in the cavities which increases the velocity of the air entering the cavities but also causes the spray sheets to draw together sooner. An equilibrium condition is arrived at whereby the air being entrained is supplied through a smaller area but at a higher velocity to a cavity at a lower pressure. Since the cavity pressure is reduced the cavitation number is no longer zero. As the speed increases further new equilibrium conditions develop but at increasing cavitation numbers.

Low speeds were considered in figure 9 to demonstrate the closure of the spray sheets. The speed range of practical interest is of course much higher. The principal data were therefore obtained at speeds between 60 and 250 fps. Figure 5 presents a typical underwater photograph from which the lengths of the cavities behind the strut were measured. Typical pressure distributions in the cavity behind the strut are presented in figure 10. The pressure decrements in the cavity with respect to the atmospheric pressure are presented as a function of the depth below the water surface in percent of submerged span. Pressure distributions are presented for three speeds: 64.5 fps, 118.2 fps, and 242.1 fps for the hydrofoil at an angle of attack of  $4^{\circ}$  and a depth of submergence of 1.0 hydrofoil chord.

The pressures in the cavity were less than atmospheric at all speeds, with the decrement increasing approximately as the square of the speed. The fact that the cavity pressures were less than atmospheric indicates that complete ventilation was not being achieved.

However, the cavity pressures were always appreciably higher than the vapor pressure of the water. This would therefore reduce the profile drag of the strut and the hydrofoil over that for the unventilated condition. The fact that the cavity pressures were decreasing with increasing speed indicates that the ratio of the air required to maintain a near-zero cavitation number to that being provided was increasing with speed. In other words the effectiveness of the ventilation in reducing the cavitation number decreased with increasing speed.

At the two lower speeds the pressure in the strut cavity was lower at the water surface than at the greater depths. This is as would be expected since as seen in figure 5 the cavity expanded below the water surface due to the increasing effective thickness of the water being deflected. The increasing cross section of the cavity formed a diffuser resulting in a pressure rise since the velocity of the ventilating air was subsonic. At the higher speed the pressure in the strut cavity was greater at the water surface than at the greater depths. This results from the fact that the pressure ratio across the spray region at the water surface was less than the critical pressure ratio and this region formed a supersonic nozzle so that the pressure decreased in the supersonic diffuser formed by the expanding cavity below the water surface.

The lowest point on the pressure distributions was obtained in the hydrofoil cavity. At the two lower speeds the pressure decrement behind the hydrofoil was greater than that behind the strut. The

opposite was the case at the higher speed. At the lower speeds for the angle of attack of  $4^{\circ}$  the hydrofoil was wetted except at the base while at the higher speed only the lower surface was wetted and a cavity extended over the upper surface from the leading edge of the hydrofoil. This change in cavity configuration probably resulted in different air entrainment conditions and a consequent different local pressure.

Computation of the apparent ratio of the spray thickness at the water surface to the strut thickness  $w/t$  from the pressure measurements and the cavity lengths at the water surface indicated in general a constant value of  $w/t$  of about 0.75 for the range of conditions investigated. For the strut used this  $w/t$  is a thickness of about 0.45 inch. While this may appear to be thick it must be realized that the transition from the horizontal water surface to the vertical spray sheet would be expected to be a concave fairing or cove. The cavity length at the apparent water surface seen by the underwater camera is in this region. Close inspection of the photograph in figure 5 shows that the cavity length appears to start a rapid decrease in length in the proximity of the apparent water surface. This would indicate that the spray sheet was thinning rapidly as would be expected if a cove were present.

Since the pressure in the strut cavity did not vary greatly with depth (see fig. 10) the change in cavity length must be primarily due to an increase in the effective thickness of the water being affected by the pressure differential and an increase in the local water velocity.

At some depth the effective thickness and the local water velocity should approach that for the infinite medium case and the cavity length should therefore approach that for the case of a two-dimensional strut. The length of a cavity for a two-dimensional strut is defined in reference 11 as

$$\frac{x}{t} = \frac{2\left(1 + \frac{\sigma}{2}\right)}{\sigma} \quad (8)$$

where  $t$  is the maximum width of the cavity which in the present case was considered to be approximated by the thickness of the parabolic strut. The length of the strut cavity where it intersected the hydrofoil cavity was, for those conditions where this length was sufficiently short to be in the field of the camera, found to be in good agreement with that predicted by reference 11. The ratio of the cavity length at the water surface measured from the photographs to the length predicted by equation (8) was in general found to be constant at a value of about 0.11 for the range of conditions investigated. The tendency for this ratio to be constant for all depths of submersion, angles of attack, and speeds is not completely understood.

No means are available to predict the cavity pressure or how it would vary with the various parameters involved. Certainly a balance between the rate at which the water entrains away the air in the cavity and the volume of air inflow permitted by the stricture formed by the spray sheets must exist. However, it seems that there may be several combinations of conditions that would provide this balance. Further

investigation will be necessary to provide a method of predicting cavitation numbers for submerged hydrofoils supported by blunt based struts. However at high speeds the cavitation number and therefore the profile drag of the strut and hydrofoil will always be reduced by ventilation even if this ventilation is not complete.

## VII METHOD OF IMPROVING VENTILATION

Since the spray sheet appears to be a primary factor in determining the extent of ventilation it would be expected that small changes in the spray sheet direction might result in large changes in the degree of ventilation. This possibility was investigated by using  $45^\circ$  triangular spray deflectors (see fig. 8) having a base of 0.2 of the strut thickness. These deflectors were installed on both sides at the aft end of the strut. They extended below the water surface a distance equal to the strut thickness and far enough above the water surface to deflect the entire spray sheet.

Figure 11 is a photograph of the effect of such strips at a speed of 16 fps. The spray was deflected the full length of the strips and a fully ventilated parabolic shaped cavity was formed to this depth behind the strut. Just below the strips a stricture was again formed in the strut cavity. Comparison with the last photograph of figure 9 shows, however, that the stricture was not nearly as severe as without the strips even at this slightly higher speed.



It is believed that a thin sheet of water that was easily deflected by the pressure differential present was formed at the discontinuity at the bottom of the strips and formed the stricture. This could be at least minimized, if not eliminated, by a warping of the strips so the deflecting angle was reduced to zero in a continuous curve. The  $45^\circ$  angle apparently was more than was required to deflect the spray and should be reduced to a minimum to reduce the profile drag of the strut. An optimum strip design would be one that had the minimum angle required to deflect the uppermost portion of the spray with this angle being reduced to zero at a rate proportional to the increase in the effective thickness of the spray sheet.

The influence of these spray strips is shown in figure 12 where pressure distributions in the cavity behind the strut are presented for similar conditions but with and without the spray deflector strips installed. The data presented in figure 12 were obtained at an angle of attack of  $8^\circ$  and the upper surface was enclosed in a cavity as at the higher speed of figure 10. With the strips installed the cavity pressure was essentially atmospheric at the water surface and was considerably closer to atmospheric pressure at the greater depths than without the strips. The cavitation number based on the cavity pressure at mean depth was 0.018 with the strips and 0.068 without the strips.

The basic pressure distribution behind the strut with and without the strips installed was the same as that for the two lower speeds in figure 10 as would be expected since the critical pressure ratio had

not been attained. The pressure decrement at the base of the hydrofoil however was, as was the case in figure 10 at the higher speed, less than that behind the strut.

#### VIII CONCLUDING REMARKS

It has been observed in experimental investigations involving ventilated flows with submerged hydrofoils that complete ventilation becomes increasingly difficult to obtain as the speed and depth of submergence of the hydrofoil are increased. An exploratory investigation of this difficulty has shown that the spray sheets that form above the water surface, on blunt struts intended to induce ventilation, are the primary cause of the limited ventilation. Because of the relatively low momentum in these spray sheets they are drawn together by small pressure differentials created by the air in the cavities being carried away by entrainment in the water.

It has been shown that the degree of ventilation can be appreciably increased by using small deflectors to apply an outward velocity to the spray sheets. However, complete ventilation was not realized and it appears such ventilation may only be possible at relatively shallow submergences.

Further investigation will be necessary to provide a method of predicting cavitation numbers for submerged hydrofoils supported by blunt-based struts.

#### REFERENCES

1. Wadlin, Kenneth L.: Mechanics of Ventilation Inception. Second Symposium on Naval Hydrodynamics, Washington, D.C., August 25-29, 1958.
2. Breslin, John P., and Skalak, Richard: Stevens Institute of Technology: Exploratory Study of Ventilated Flows About Yawed Surface-Piercing Struts. NASA MEMO 2-23-59W, 1959.
3. Perry, Byrne: Experiments on Struts Piercing the Water Surface. CIT Rep. E-55.1, 1954.
4. Kiceniuk, Taras: A Preliminary Experimental Study of Vertical Hydrofoils of Low Aspect Ratio Piercing a Water Surface. CIT Rep. E-55.2, 1954.
5. Wetzel, J. M.: Experimental Studies of Air Ventilation of Vertical, Semi-Submerged Bodies. St. Anthony Falls Hydraulic Laboratory, Univ. of Minn., 1957.
6. Hay, Donald A.: Flow About Semi-Submerged Cylinders of Finite Length. Princeton Univ., 1947.
7. Wadlin, Kenneth L., Ramsen, John A., and Vaughan, Victor L., Jr.: The Hydrodynamic Characteristics of Modified Rectangular Flat Plates Having Aspect Ratios of 1.00, 0.25, and 0.125 and Operating Near a Free Water Surface. NACA Rep. 1246, 1955.

8. Vaughan, Victor L., Jr., and Ramsen, John A.: Hydrodynamic Characteristics Over a Range of Speeds Up to 80 Feet Per Second of a Rectangular Modified Flat Plate Having an Aspect Ratio of 0.25 and Operating at Several Depths of Submersion. NACA TN 3908, 1957.
9. Ramsen, John A.: An Experimental Hydrodynamic Investigation of the Inception of Vortex Ventilation. NACA TN 3903, 1957.
10. Johnson, Virgil E., Jr.: Theoretical and Experimental Investigation of Arbitrary Aspect Ratio, Supercavitating Hydrofoils Operating Near the Free Water Surface. NACA RM L57I16, 1957.
11. Tulin, M. P.: Steady Two-Dimensional Cavity Flows About Slender Bodies. DIMB Report 834, 1953.

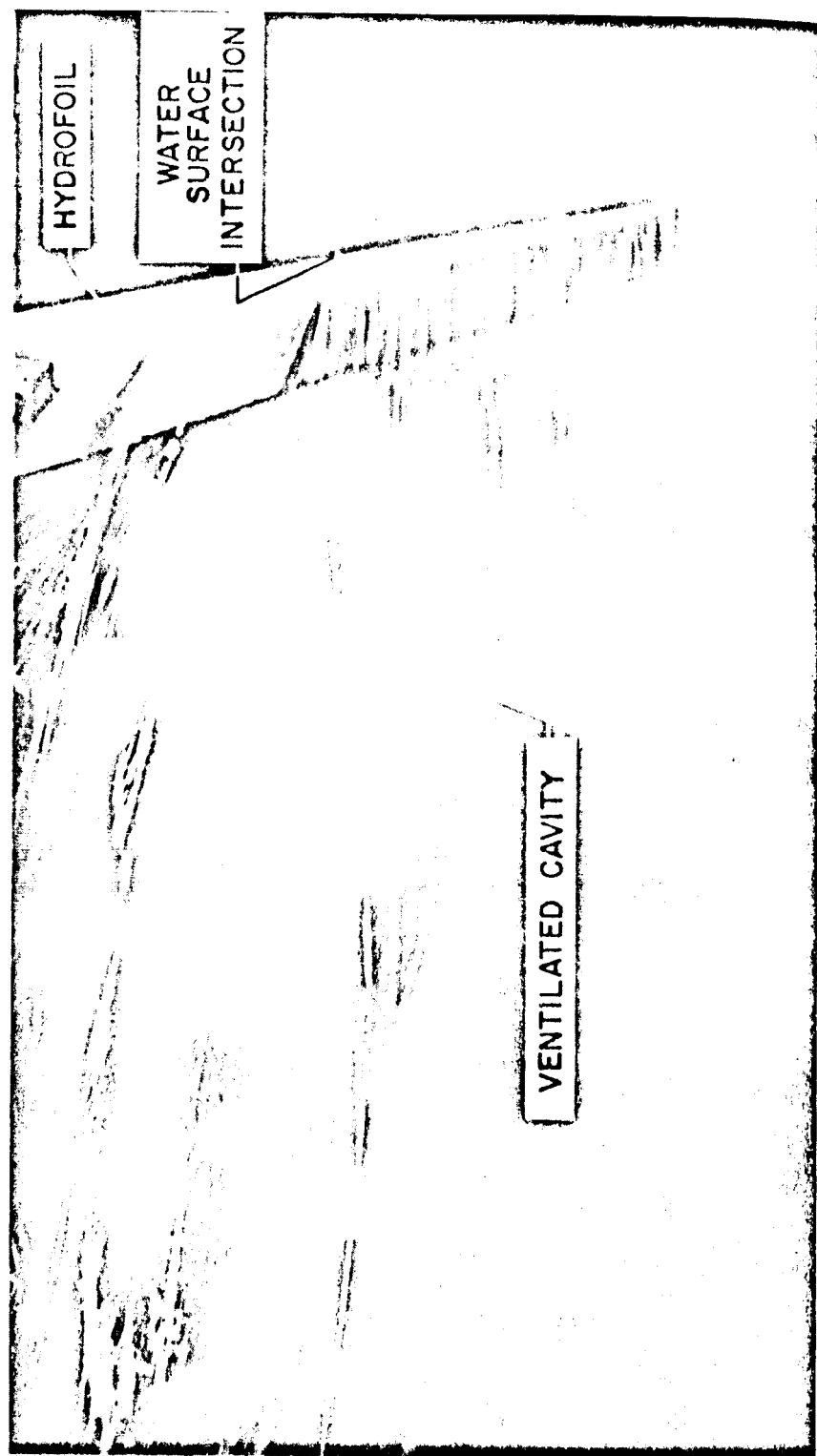
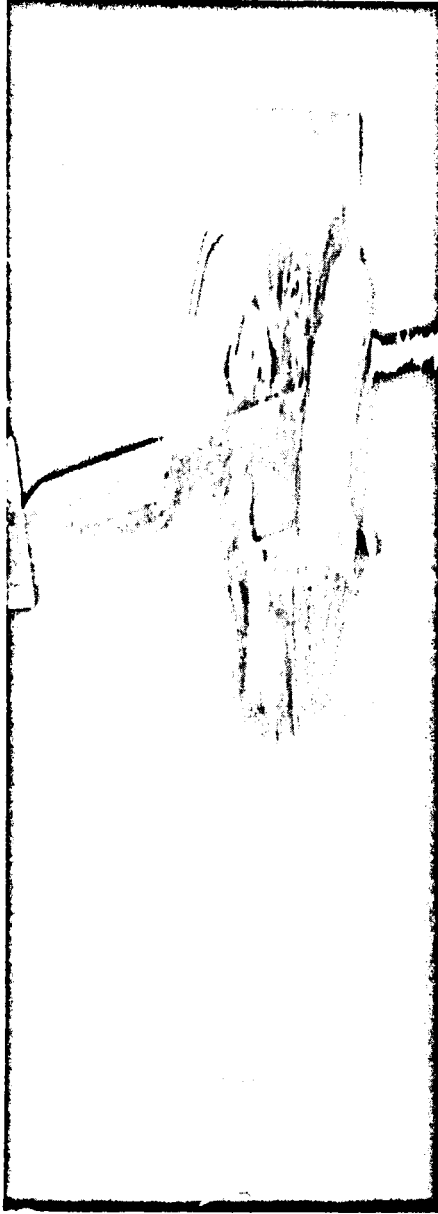


Figure 1.- Photograph of a surface-piercing hydrofoil ventilated to the atmosphere.  
L-58-2502



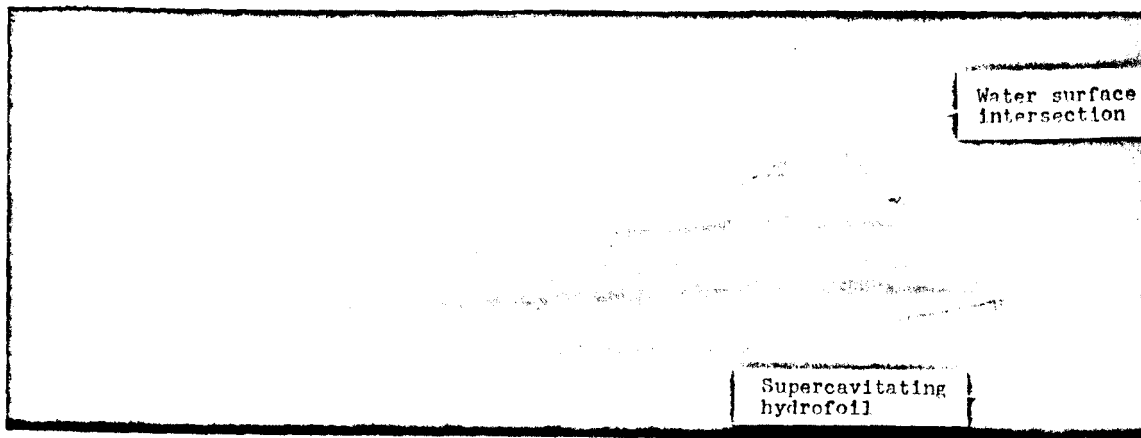
Venting of vortex



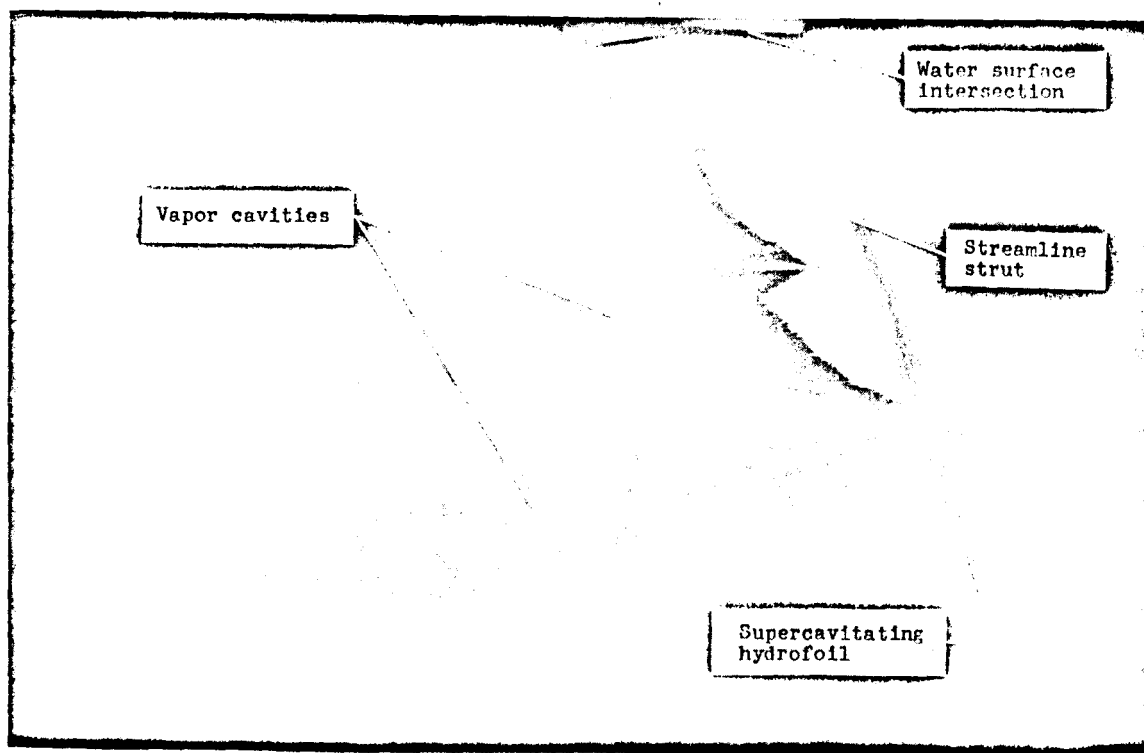
Complete ventilation

L-58-2505

Figure 2.- Photographs showing the development of vortex ventilation on an aspect-ratio-0.25 flat plate.



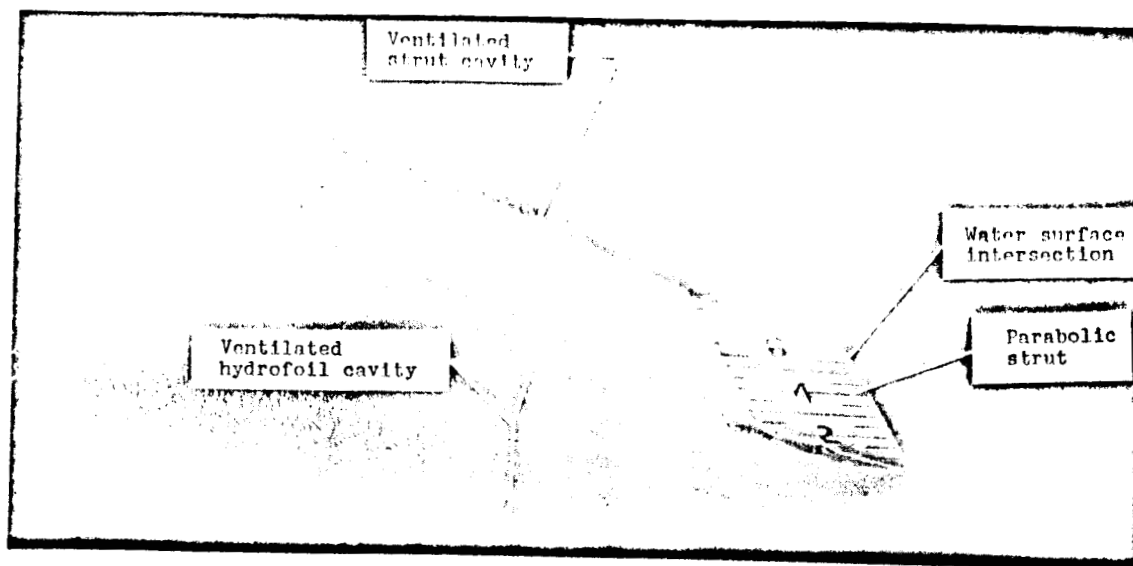
(a) Above water view.



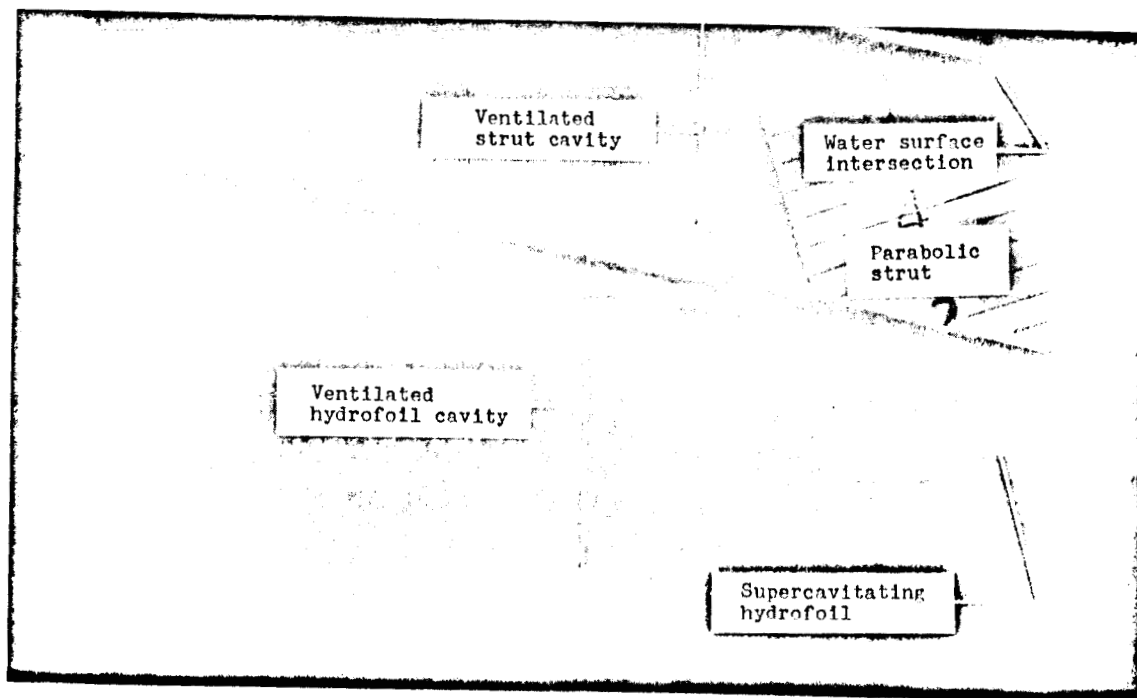
(b) Underwater side view.

L-59-3083

Figure 3.- Photographs of hydrofoil and streamline strut with vapor cavities.



(a) Above water view.



(b) Underwater side view.

L-59-3084

Figure 4.- Photographs of hydrofoil and blunt-based strut with ventilated cavities.



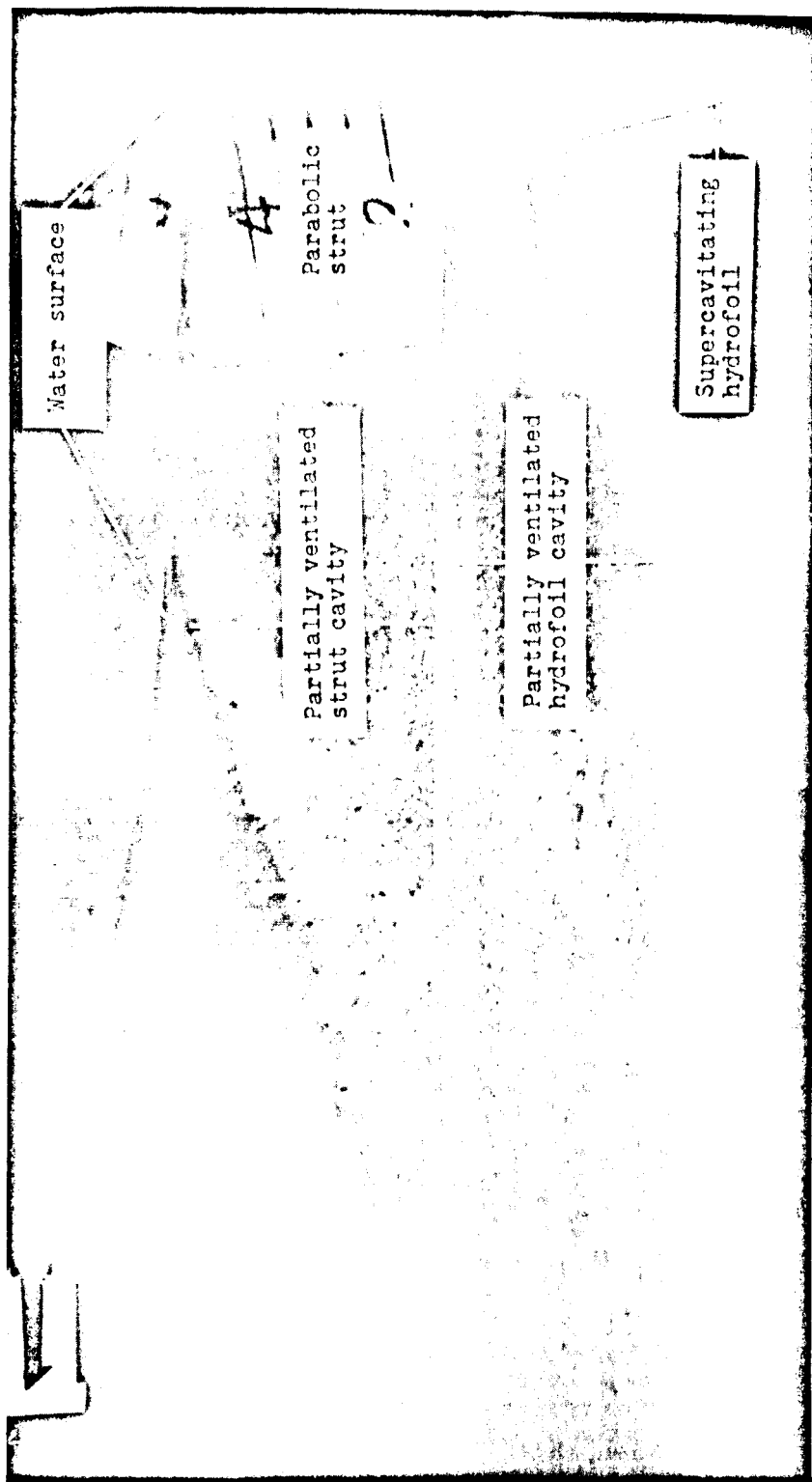


Figure 5.- Photographs of hydrofoil and blunt-based strut with partially ventilated cavities.

L-59-3085

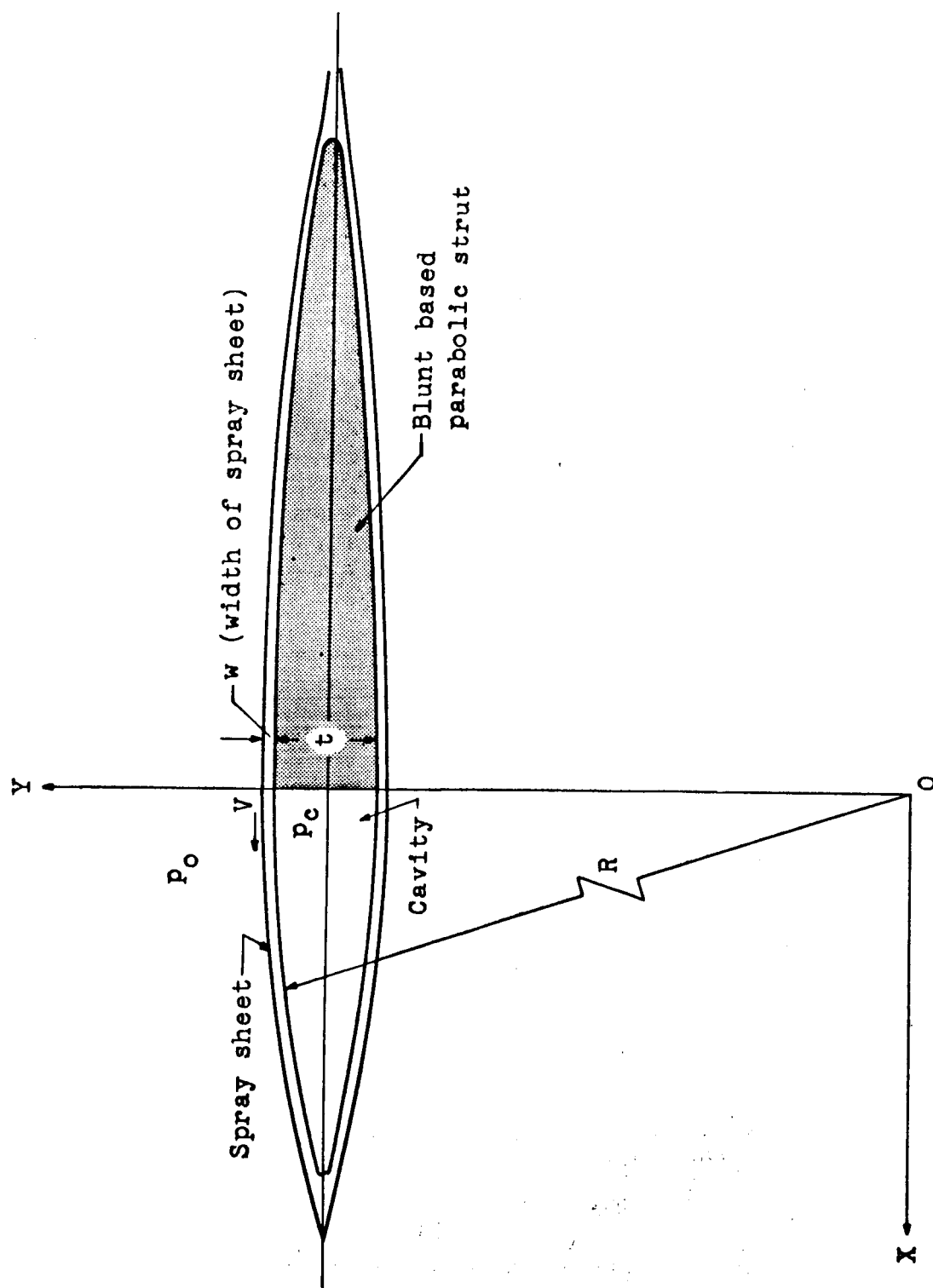


Figure 6.- Definition of spray sheet closure parameters.

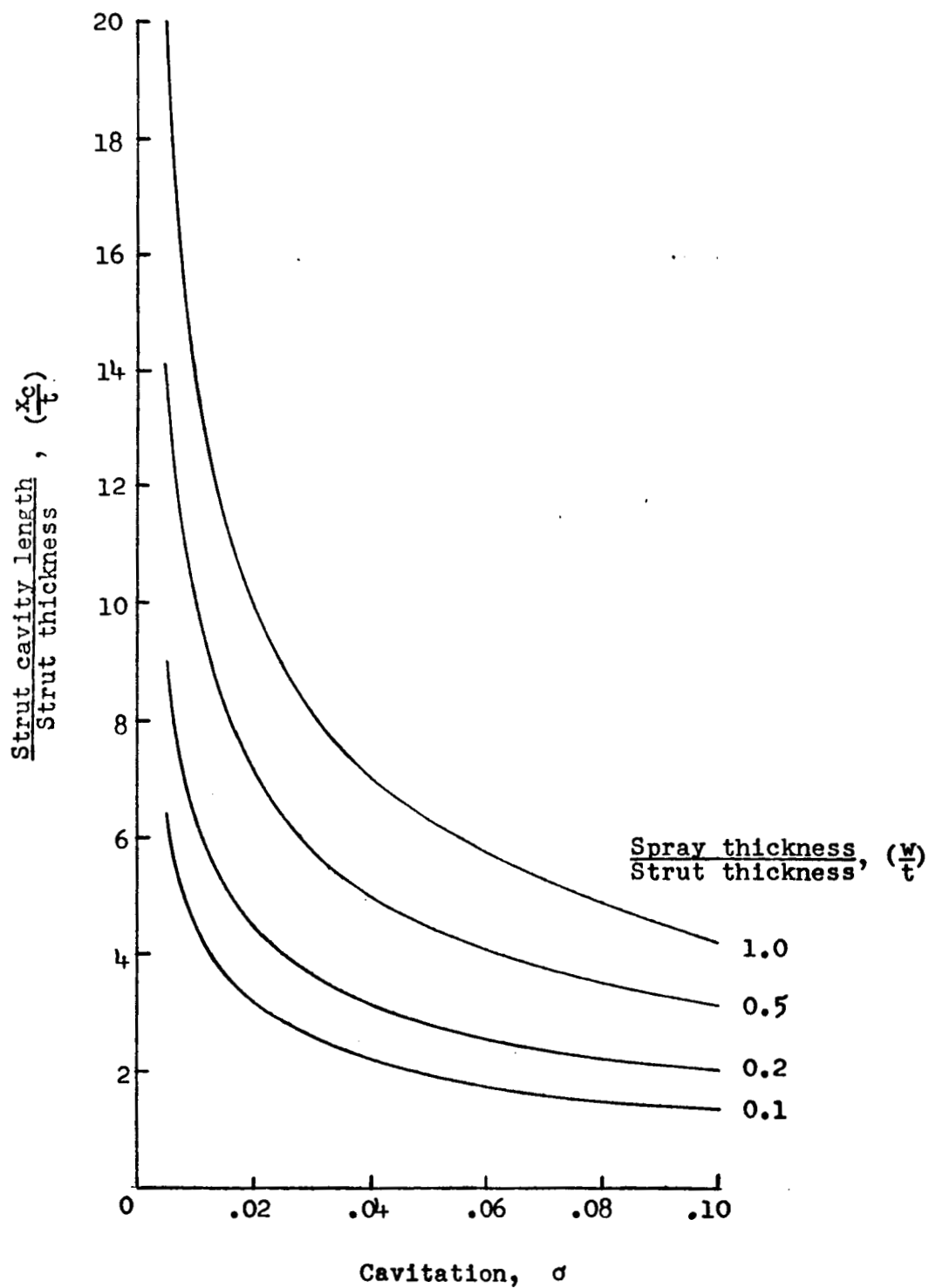


Figure 7.- Variation of strut cavity length with spray thickness and cavitation number.

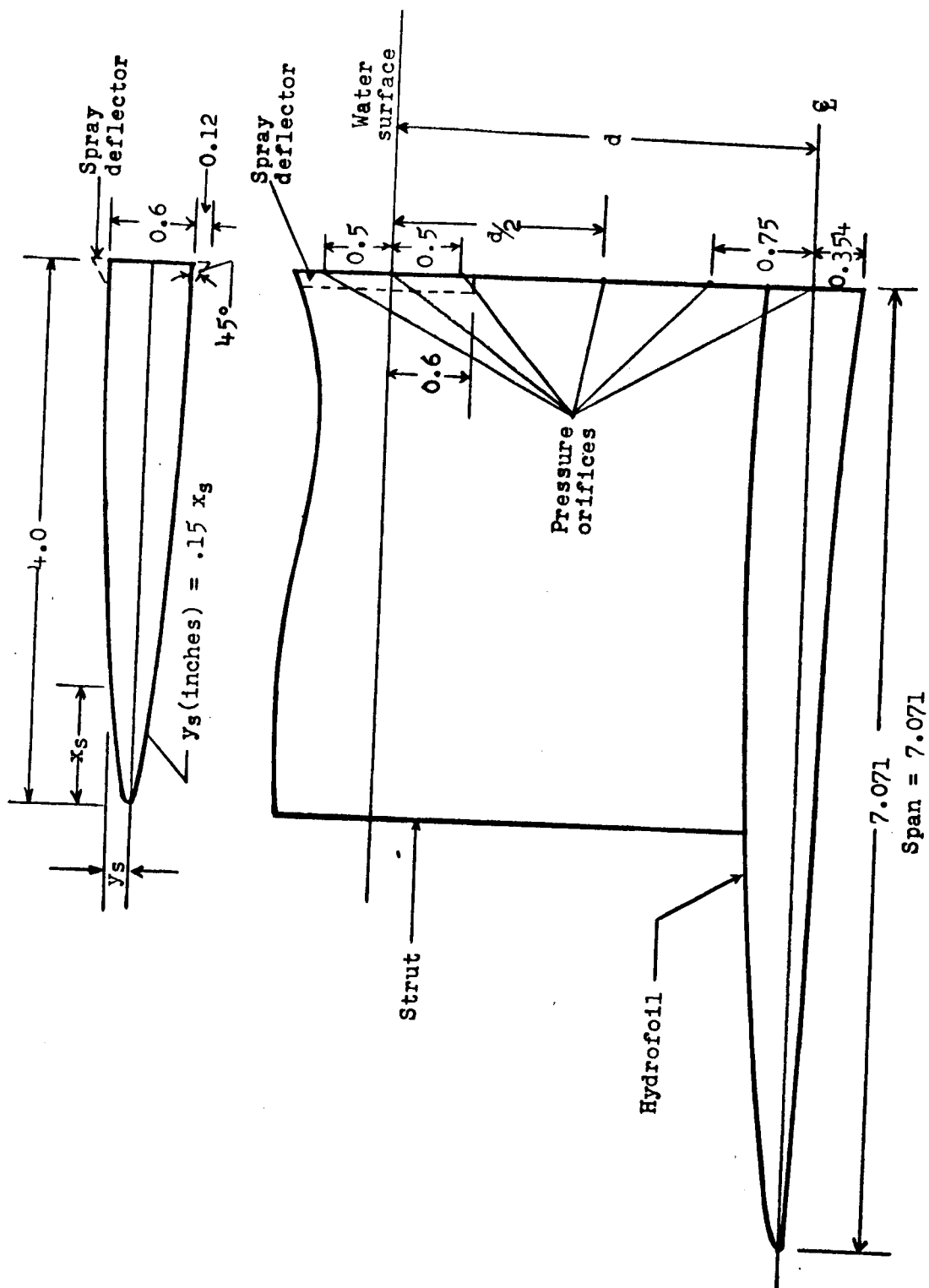
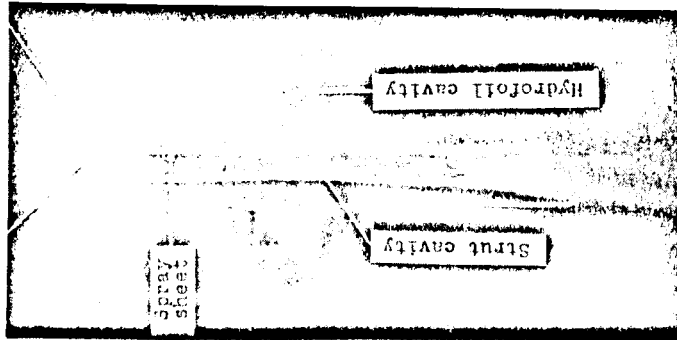
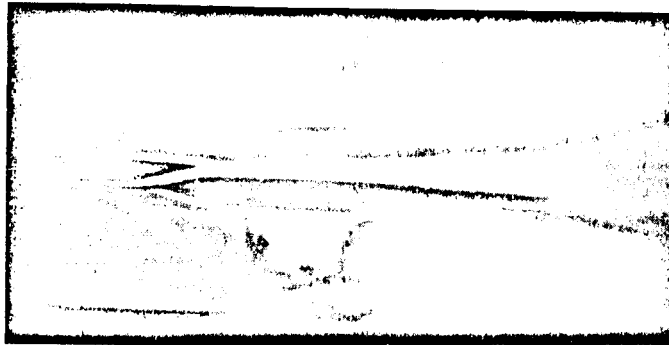


Figure 8.- Details of hydrofoil, strut, and pressure-orifice locations. (All dimensions are in inches.)

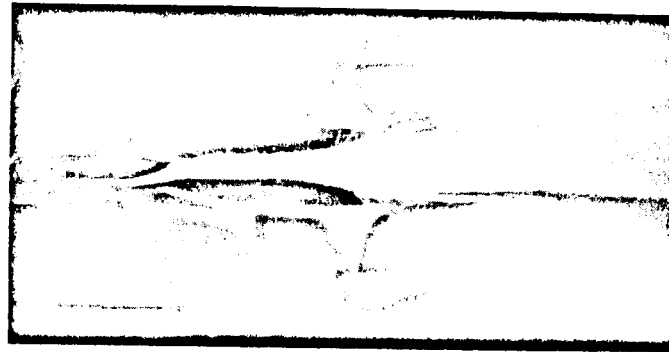
Base of strut      Hydrofoil



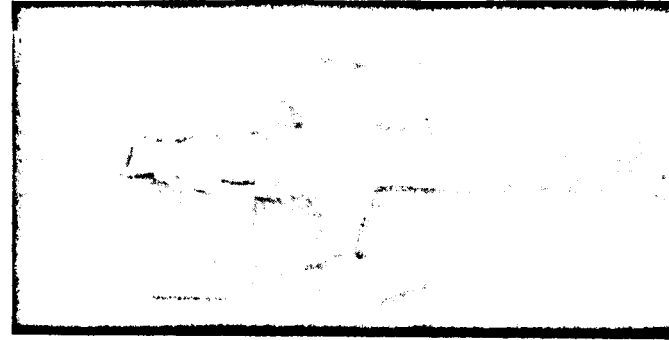
12 fps



13 fps



14 fps



15 fps

Figure 9.- Photographs showing closure of spray sheet. L-59-3086

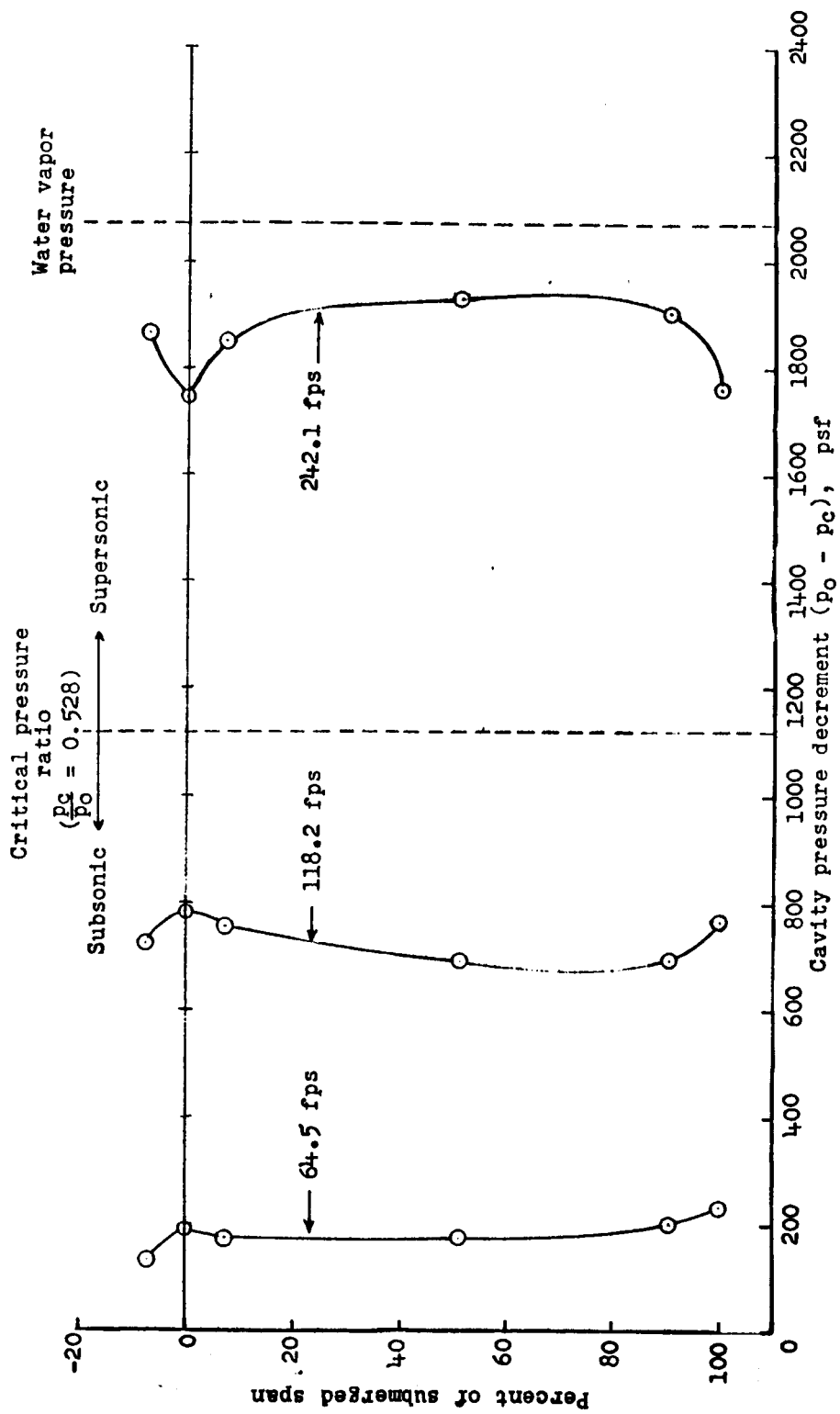
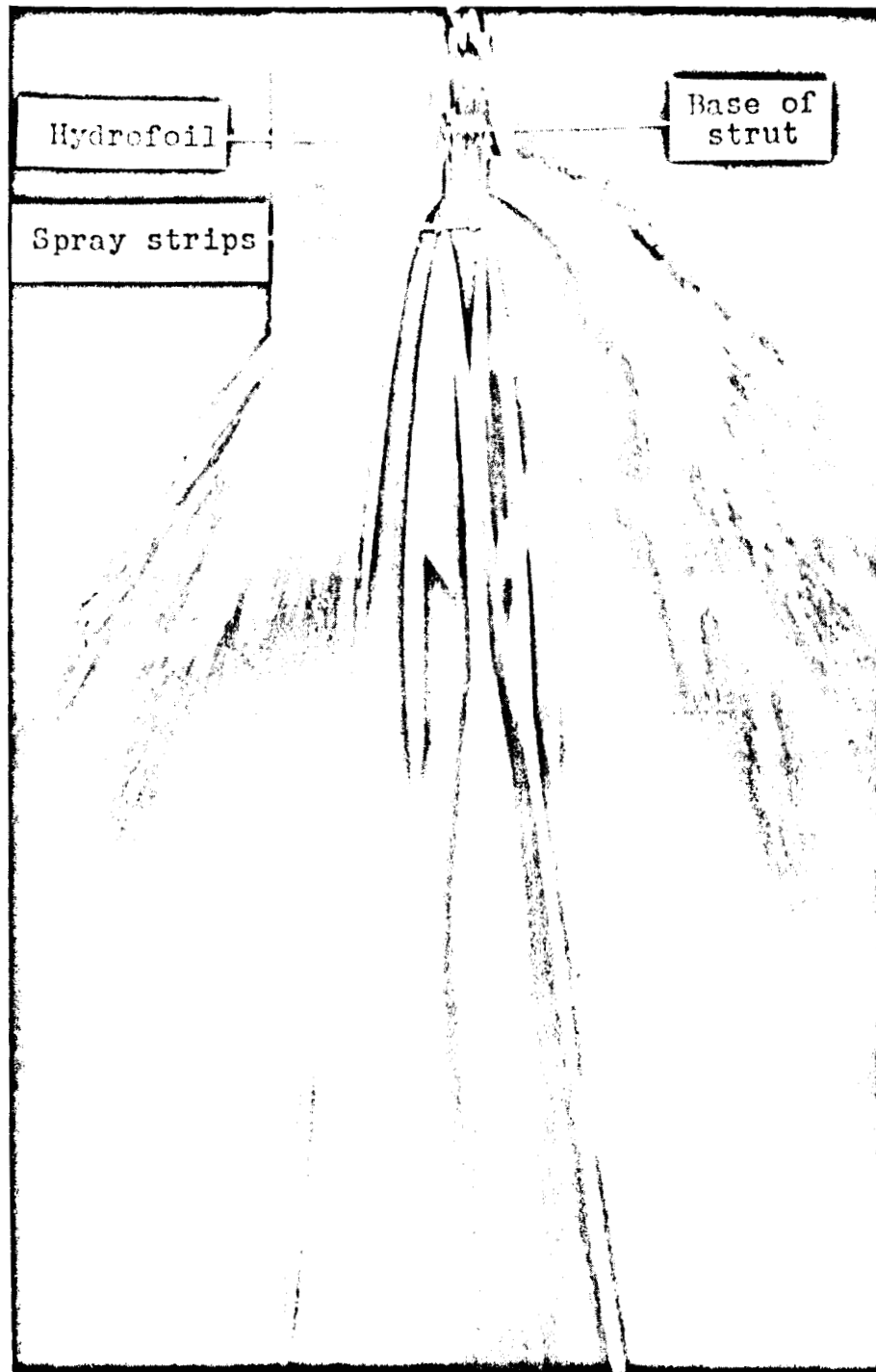


Figure 10.- Spanwise pressure distribution on strut base. (Hydrofoil angle of attack =  $4^\circ$ ; depth of submergence - one hydrofoil chord.)



L-59-3087  
Figure 11.- Photograph of spray sheet with spray deflecting strips.

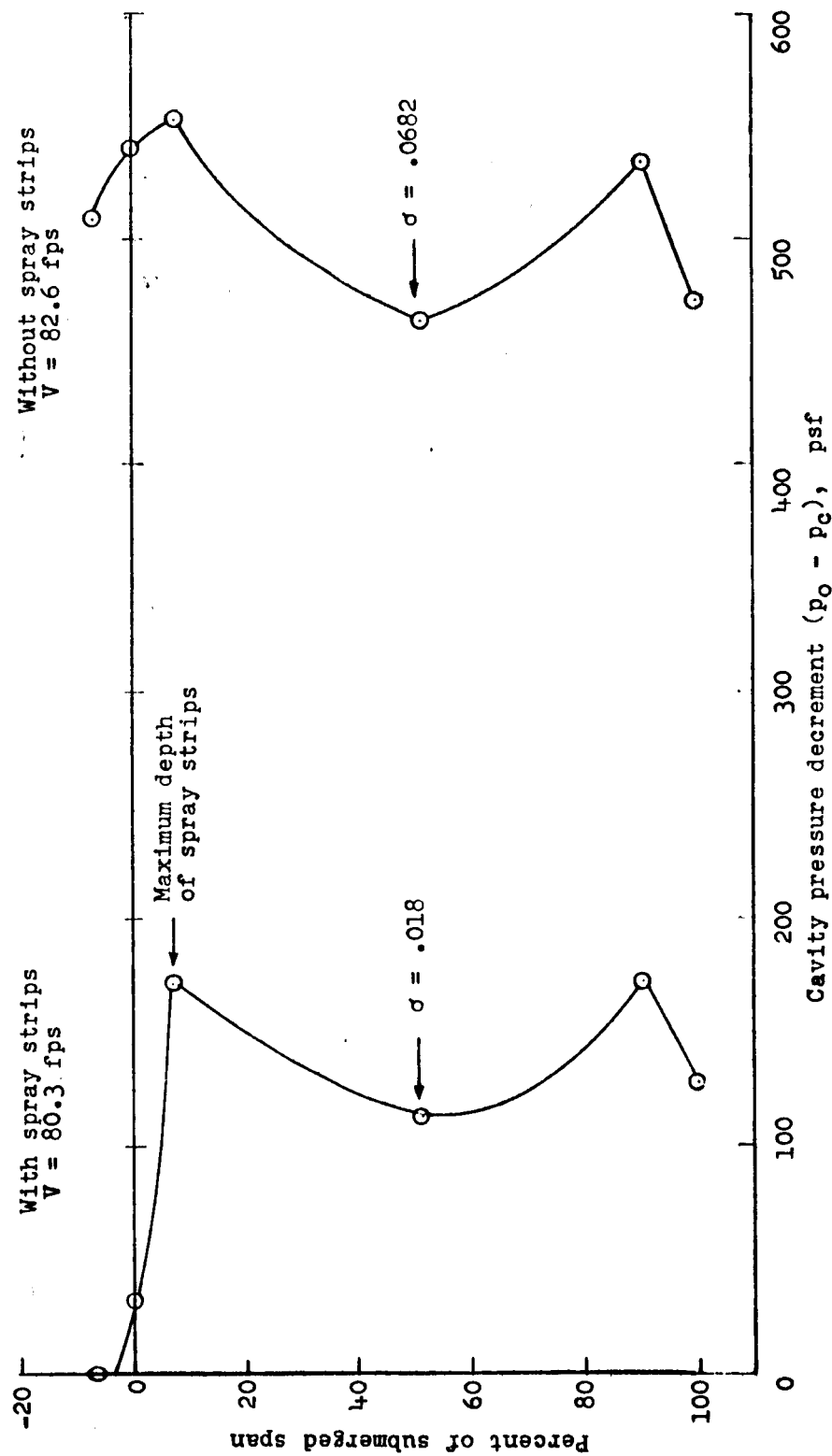


Figure 12.- Effect of spray strips on the spanwise pressure distribution on strut base.  
(Hydrofoil angle of attack =  $8^\circ$ ; depth of submergence - one hydrofoil chord.)